



Open Access

INVITED ORIGINAL ARTICLE

Male Fertility

CRISPR/Cas9-mediated genome editing reveals 12 testis-enriched genes dispensable for male fertility in mice

Yuki Oyama^{1,2}, Haruhiko Miyata², Keisuke Shimada², Yoshitaka Fujihara^{2,3}, Keizo Tokuhira⁴, Thomas X Garcia^{5,6,7}, Martin M Matzuk^{5,6}, Masahito Ikawa^{1,2,8}

Gene expression analyses suggest that more than 1000–2000 genes are expressed predominantly in mouse and human testes. Although functional analyses of hundreds of these genes have been performed, there are still many testis-enriched genes whose functions remain unexplored. Analyzing gene function using knockout (KO) mice is a powerful tool to discern if the gene of interest is essential for sperm formation, function, and male fertility *in vivo*. In this study, we generated KO mice for 12 testis-enriched genes, *1700057G04Rik*, *4921539E11Rik*, *4930558C23Rik*, *Cby2*, *Ldhal6b*, *Rasef*, *Slc25a2*, *Slc25a41*, *Smim8*, *Smim9*, *Tmem210*, and *Tomm20l*, using the clustered regularly interspaced short palindromic repeats /CRISPR-associated protein 9 (CRISPR/Cas9) system. We designed two gRNAs for each gene to excise almost all the protein-coding regions to ensure that the deletions in these genes result in a null mutation. Mating tests of KO mice reveal that these 12 genes are not essential for male fertility, at least when individually ablated, and not together with other potentially compensatory paralogous genes. Our results could prevent other laboratories from expending duplicative effort generating KO mice, for which no apparent phenotype exists.

Asian Journal of Andrology (2022) 24, 266–272; doi: 10.4103/aja.aja_63_21; published online: 16 July 2021

Keywords: CRISPR/Cas9; knockout mice; male infertility; spermatozoa; testis

INTRODUCTION

Fertilization is the union of two gametes, spermatozoa and eggs, which conveys their genetic information to the next generation. Abnormal formation or function of these gametes leads to infertility with male factors contributing to nearly 50% of overall cases.^{1,2} Spermatozoa, male haploid gametes, are produced through spermatogenesis in the seminiferous tubules of the testis. During spermatogenesis, diploid spermatocytes undergo meiosis to produce round spermatids and then go through spermiogenesis that is the acquisition of specialized morphology and function. During spermiogenesis, round spermatids pack their haploid genome to form the sperm heads that contain an exocytotic vesicle called the acrosome, and they generate thread-like flagella that function as the motility apparatus for the resulting spermatozoa.^{3–5}

Knockout (KO) mice are widely used to understand male fertility *in vivo* because there is no culture system that produces fully functional spermatozoa *in vitro*. KO mice provide a clear answer to whether or not a gene of interest is essential for male fertility, and because of the high sequence similarity between mouse and human genomes, also provide profound insight into the potential physiological function and

functional requirement of the orthologous genes in human. Previously, it has been time consuming and costly to generate KO mice with the conventional method that utilizes homologous recombination in embryonic stem cells and subsequent generation of chimeric mice, but the emergence of genome editing technology such as the clustered regularly interspaced short palindromic repeats/CRISPR-associated protein 9 (CRISPR/Cas9) system makes it possible to generate KO mice in a short period of time with relatively low costs, which can be utilized in the field of andrology as well.⁶

In mice and humans, it has been reported that more than 1000–2000 genes are expressed predominantly in the testis.^{7–9} These genes are speculated to play essential roles in sperm formation and/or function because of their restricted expression in the testes. While a considerable number of these genes have been discovered over the years to be essential for male fertility,^{6,10} an even greater number of these genes have been found to be not essential for male fertility *per se*, which might be due to functional redundancy.^{8,11–15} Of note, we recently reported that four genes (fertilization-influencing membrane protein [*Fimp*], sperm–oocyte fusion required 1 [*Sof1*], transmembrane protein 95 [*Tmem95*], and sperm acrosome associated 6 [*Spaca6*]) are

¹Graduate School of Pharmaceutical Sciences, Osaka University, Suita, Osaka 565-0871, Japan; ²Department of Experimental Genome Research, Research Institute for Microbial Diseases, Osaka University, Suita, Osaka 565-0871, Japan; ³Department of Bioscience and Genetics, National Cerebral and Cardiovascular Center, Suita, Osaka 564-8565, Japan; ⁴Department of Genome Editing, Institute of Biomedical Science, Kansai Medical University, Hirakata, Osaka 573-1191, Japan; ⁵Center for Drug Discovery, Baylor College of Medicine, Houston, TX 77030, USA; ⁶Department of Pathology and Immunology, Baylor College of Medicine, Houston, TX 77030, USA; ⁷Department of Biology and Biotechnology, University of Houston–Clear Lake, Houston, TX 77058, USA; ⁸The Institute of Medical Science, The University of Tokyo, Minato-ku, Tokyo 108-8639, Japan.

Correspondence: Dr. H Miyata (hmiya003@biken.osaka-u.ac.jp) or Dr. M Ikawa (ikawa@biken.osaka-u.ac.jp)

Received: 24 March 2021; Accepted: 26 May 2021

essential for sperm–egg fusion,^{16–18} which is astonishing considering that no other male factors essential for fusion have been found for 15 years since izumo sperm–egg fusion 1 (IZUMO1), the first male fusion factor, was discovered.¹⁹ These results indicate that screening testis-enriched genes in an organismal model with the CRISPR/Cas9 system is imperative to identify not only genes dispensable for male fertility but also genes that play critical roles in sperm formation and/or function.

Here, we deleted 12 mouse genes that are predicted to be expressed predominantly in the testis with the CRISPR/Cas9 system and revealed that all 12 genes were dispensable for male fertility. These data could prevent unnecessary expenditures and efforts by others.

MATERIALS AND METHODS

Animals

All animal experiments performed in this study were approved by the Institutional Animal Care and Use Committees of Osaka University (Osaka, Japan), National Cerebral and Cardiovascular Center (Osaka, Japan), and Kansai Medical University (Osaka, Japan) in compliance with the guidelines and regulations for animal experiments. In this study, all B6D2F1 and ICR mice were purchased from CLEA Japan, Inc. (Tokyo, Japan), Japan SLC, Inc. (Shizuoka, Japan), or Shimizu Laboratory Supplies (Kyoto, Japan).

Digital PCR

Digital PCRs (heatmaps) depicting average transcript per million values across various mouse and human reproductive and nonreproductive tissues were conducted as previously performed using our previously reported data.¹⁵ Briefly, sequences for different tissues were downloaded from Sequence Read Archives, trimmed using TrimGalore, and aligned to the human genome (GRCh38) or mouse genome (GRCm38) by HISAT2.²⁰ Feature Counts was used to quantify gene expression in each tissue, and RUVr²¹ was used to batch correct tissues by removing unwanted variation. EdgeR was used to determine differential gene expression for each nonreproductive tissue against each reproductive tissue.²²

Reverse transcription PCR (RT-PCR)

Mouse cDNA was prepared from multiple adult tissues of C57BL/6N using TRIzol (Thermo Fisher Scientific, Waltham, MA, USA) according to the manufacturer's protocol. The obtained RNA was immediately reverse transcribed to cDNA with SuperScript IV first-strand synthesis system (Thermo Fisher Scientific) using oligo (dT) as primers. PCR primers and amplification conditions for each gene are shown in **Supplementary Table 1**.

Phylogenetic analysis

The phylogenetic trees of candidate genes were created using the neighbor-joining method with the GENETYX software (GENETYX, Tokyo, Japan). For the amino acid sequences, we chose cattle, dog, horse, human, mouse, and pig for mammals and chicken for birds.

Generation of KO mice with the CRISPR/Cas9 system

All KO mouse lines in this study were produced with the CRISPR/Cas9 system. CRISPRdirect software was used to find off-target sequences when we chose gRNAs (**Table 1**).²³ To generate KO mice, we performed electroporation using zygotes as described previously.^{24,25} Cas9 protein (Thermo Fisher Scientific or Integrated DNA Technologies, Coralville, IA, USA) was mixed with crRNAs, tracrRNA (Integrated DNA Technologies or Merck, Darmstadt, Germany), and Opti-MEM (Thermo Fisher Scientific). This solution was incubated at 37°C to

generate the gRNA/Cas9 ribonucleoprotein (RNP) complex, and the obtained complex was electroporated into fertilized oocytes using NEPA21 Super Electroporator (Nepagene, Chiba, Japan). The treated embryos that developed to the 2-cell stage were transplanted into the oviducts of pseudopregnant ICR females at 0.5 days after mating with vasectomized males. Pups were obtained by natural or cesarean section, and subsequent sibling crosses were performed to obtain homozygous KO mice. Genotyping was performed through PCR using primers listed in **Supplementary Table 2**. All gene-modified mice generated in this study will be made available to other investigators through either the RIKEN BioResource Research Center, Tsukuba, Ibaraki, Japan, or the Center for Animal Resources and Development (CARD), Kumamoto University, Kumamoto, Japan.

Morphological and histological analysis of testes

After euthanasia, testes were dissected. After measuring the testicular weight, the testes were fixed in Bouin's solution (Polysciences, Warrington, PA, USA), embedded in paraffin, sectioned at a thickness of 5 µm on a Microm HM325 microtome (Microm, Walldorf, Germany), rehydrated, and treated with 1% periodic acid for 10 min, followed by treatment with Schiff's reagent (FUJIFILM Wako, Osaka, Japan) for 20 min. The sections were then stained with Mayer's hematoxylin solution (FUJIFILM Wako) before imaging and observed using an Olympus BX53 microscope equipped with an Olympus DP74 color camera (Olympus, Tokyo, Japan).

Analysis of morphology and motility of spermatozoa

Spermatozoa from cauda epididymis were suspended in TYH medium,²⁶ incubated at 37°C for either 10 min or 120 min, diluted, and then placed on MAS-coated glass slides (Matsunami Glass, Osaka, Japan) for morphology assessment using an Olympus BX53 microscope or placed in glass chambers for sperm motility analysis using the CEROS II sperm analysis system (software version 1.5; Hamilton Thorne Biosciences, Beverly, MA, USA).

Fertility analysis of KO lines

Sexually mature wild type (WT) or KO male mice were caged individually with one to three six-week-old female mice for at least eight weeks (except for small integral membrane protein 8 [*Smim8*]). Male mice were removed after the mating period, and females were kept for another three weeks to count the final litters. The numbers of pups and copulation plugs were counted every morning.

Statistical analyses

Statistical difference was determined using the Welch's *t*-test by Microsoft Office Excel (Microsoft Corporation, Redmond, WA, USA). Differences were considered statically significant if the $P < 0.05$. Data represent the mean ± standard deviation (s.d.).

RESULTS

Expression patterns of candidate genes in mouse and human

To examine the mouse and human reproductive and nonreproductive tissue expression patterns of the 12 genes in this study, we performed digital PCR as described.¹⁵ Except for lactate dehydrogenase A-like 6B (*Ldhal6b*) and small integral membrane protein 9 (*Smim9*), all genes exhibited enriched expression in mouse testis (**Figure 1a**). Because no data were found for *Ldhal6b* and whole tissue expression signal was weak for *Smim9* in the digital PCR, we performed RT-PCR for *Ldhal6b* and *Smim9* using mouse tissues and found that the expression of both genes was enriched in the testis (**Figure 1b**). Further, we confirmed the expression of these genes in human testis with digital PCR (**Figure 1c**),

Table 1: The sequences of guide RNA and deleted regions

Gene symbol	Guide RNAs	CRISPR/Cas9 efficiency, n/total (%)	CRISPR/Cas9 delivered gene deletion (intron, exon) ^a	Mutation (bp)
<i>1700057G04Rik</i>	Up: TTAGGATATCATCTAAACT Down: GAAACATCTGGAACAGCT	10/18 (55.6)	Up: gcttcttaggatcatctaaact Down: tagtctccagaaacatctggaaca	-3950
<i>4921539E11Rik</i>	Up: TACCTGGAGCAGTAATAGAG Down: ACCCATTGGATAACCTGCT	1/6 (16.7)	Up: gagaggaactctccccttatgccta Down: AACAACATGACCCATTGGATAACC	-53 580
<i>4930558C23Rik</i>	Up: CAGACACAGCTACCTCCAGC Down: ACCCAGGGACATAAGATAT	6/22 (27.3)	Up: GAGGTAGCTGTGCTGGAAGACAGT Down: ggctatgatgttcaattgtccata	-597
<i>Cby2</i>	Up: CTGACTCTGGCTAGCCACGT Down: GCCCAGAAGCACGTGCCCGT	5/12 (41.7)	Up: gggcacagcagcagcaaccaatcc Down: ACTCTGCCCAGAAGCACGTGCCCGT	-10 210
<i>Ldhal6b</i>	Up: CCTAGCAACGGCCGCCGTG Down: GAAGCGGGGTTCCGAAAGC	3/22 (13.6)	Up: GTTGTGGCCTCAACTGTCTTCCTCA Down: TGTGGGGTGAAGCGGGGTTCCGAA	-1281
<i>Rasef</i>	Up: AGCATGACTTCTGTGGCG Down: GCTTCAGTTGCTGAGAGCG	8/19 (42.1)	Up: acgccacaaggaagtcatgtagt Down: GTTCTTCCCCTCTCAGCAACCTG	-63 153
<i>Slc25a2</i>	Up: CAGTGAGTCTATGGCGCT Down: AGGGATGGCTCGAATCAGAG	5/15 (33.3)	Up: CGCCATAGACTACTGCGGGCGCA Down: ATTCTGGATTGAAAGCCACTCTGAT	-795+1
<i>Slc25a41</i>	Up: TTATCCAGCCTTGCGTTTA Down: ACTCGGATTAGAAAAGCGCT	6/16 (37.5)	Up: ACCGCAAGGCTGGATAACCAGCCAC Down: CACCCAGGACTCGGATTAGAAAAGC	-8811
<i>Smim8</i>	Up: TGGTTGTGTGCGCCCTCGG Down: GTGAAGGCATCGGTACATG	8/11 (72.7)	Up: CGCACACAACCACCTATTTCGAGC Down: GTGAAGGCATCGGTACATGAGGAG	-2300
<i>Smim9</i>	Up: CCTCTGAAGCTGTTCTGCAT Down: GAAAATTCTGGAATCCTACT	29/39 (74.4)	Up: CATAGGACTGCTCTGTGCCCTCTG Down: TGAATCTAATCAAGgtctgctag	-12 405
<i>Tmem210</i>	Up: TTCCAATGAGTTCATCTAG Down: GTAGTGGAGGCAACTAGGG	7/9 (77.8)	Up: TAGAGGTGTGTGGTGGGGTTGGGGG Down: TTCCACAGTAGTGGAGGCAACTAG	-1016
<i>Tomm20l</i>	Up: TGCAGTGTCTTGGGTGCGC Down: GAGGTGCAGCAGCCGCCA	3/9 (33.3)	Up: gaaatccaggcagcaaggacact Down: gtgaggtgcagcagaccgcaagg	-483

^aUppercases indicate exon sequences and lowercases indicate intron sequences. CRISPR/Cas9: clustered regularly interspaced short palindromic repeats/CRISPR-associated protein 9; *Cby2*: chibby family member 2; *Ldhal6b*: lactate dehydrogenase A-like 6B; *Rasef*: RAS and EF hand domain containing; *Slc25a2*: solute carrier family 25 member 2; *Slc25a41*: solute carrier family 25 member 41; *Smim8*: small integral membrane protein 8; *Smim9*: small integral membrane protein 9; *Tmem210*: transmembrane protein 210; *Tomm20l*: translocase of outer mitochondrial membrane 20-like. CRISPR/Cas9 efficiency was calculated by the number of mutant pups divided by the number of genotyped pups. CRISPR/Cas9 delivered gene deletion indicates 25 bp sequences upstream and downstream of the deleted regions

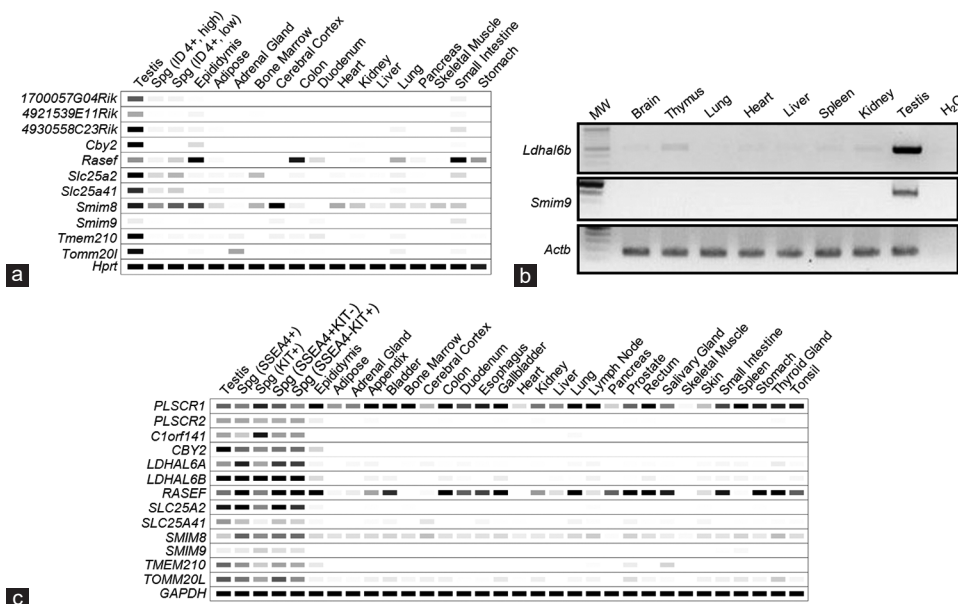


Figure 1: Expression patterns of specific genes in various tissues. (a) Digital PCR shows the average transcripts per million (TPM) value per tissue per gene from published mouse RNA-seq datasets.¹⁵ White = 0 TPM, Black ≥ 30 TPM. *Hprt* expression is shown as housekeeping control. (b) Expression patterns of *Ldhal6b* and *Smim9* in mouse tissues using RT-PCR. *Actb* expression is shown as housekeeping control. MW: molecular weight marker. (c) Digital PCR shows the average TPM value per tissue from published human RNA-seq datasets.¹⁵ *PLSCR1* and *PLSCR2* are orthologs of mouse *1700057G04Rik*. *C1orf141* is an ortholog of mouse *4921539E11Rik*. White = 0 TPM, Black ≥ 30 TPM. *GAPDH* expression is shown as housekeeping control. RT-PCR: reverse transcription PCR; *Hprt*: hypoxanthine guanine phosphoribosyl transferase; *Actb*: actin beta; *C1orf141*: chromosome 1 open reading frame 141; *GAPDH*: glyceraldehyde-3-phosphate dehydrogenase; *PLSCR1*: phospholipid scramblase 1; *PLSCR2*: phospholipid scramblase 2. The expansions of the other genes have been described in the notes of Table 1.

although there were no expression data for cortixin domain containing 2 (*CTXND2*), the human homolog of *4930558C23Rik*. All the genes were conserved in humans (Supplementary Figure 1).

Generation of KO mice

To investigate the function of candidate genes in male reproduction, the 12 genes were ablated individually using the CRISPR/Cas9 system. For each of the genes, either the entire protein coding region or almost all of the protein coding regions were deleted through nonhomologous end joining to ensure that each gene was completely ablated and that no partially functional transcript may still be expressed (Supplementary Figure 2). Genome-editing efficiency (the number of mutant pups divided by the total number of genotyped pups) ranged from 13.6% to 77.8%. The efficiency of genome-editing and mutation details are summarized in Table 1.

Phenotypic analysis of *4921539E11Rik*, *4930558C23Rik*, and transmembrane protein 210 (*Tmem210*) KO mouse lines

Herein, as an example of *in vivo* functional analysis, we performed a detailed phenotypic analysis on three KO lines: *4921539E11Rik*, *4930558C23Rik*, and *Tmem210* (Figure 2–4).

4921539E11Rik KO mice were generated using two gRNAs designed upstream of the start codon in intron 1 and near the stop codon in exon 9 (Figure 2a). Their genotypes were confirmed by genomic PCR (Figure 2b) using primers shown in Figure 2a. Sanger sequencing

showed that the KO mouse had a 53 580 bp deletion (Figure 2b). Homozygous KO mice were viable and no overt abnormalities were found. There were no significant differences in the testis appearance (Figure 2c), testis weight (Figure 2d), and testis histology (Figure 2e). Further, we found no overt abnormalities in sperm morphology (Figure 2f). We also checked the percentage of motile spermatozoa using the computer-assisted sperm analysis (CASA) system and found no differences between the control and KO mice (Figure 2g).

To disrupt *4930558C23Rik*, we designed two gRNAs, one before the start codon and the second after the stop codon of exon 2 (Figure 3a). To identify the mutant allele, we performed PCR using primers presented in Figure 3a. The resulting mutant allele carrying a 597-bp deletion was identified by PCR and Sanger sequencing (Figure 3b). *4930558C23Rik* KO mice exhibited normal testicular size (Figure 3c and 3d) and histology (Figure 3e). Further, sperm morphology and percentage of motile spermatozoa analyzed with the CASA system were comparable between the control and KO mice (Figure 3f and 3g).

Tmem210 was mutated using two gRNAs, one upstream of exon 1 and the other near the stop codon of exon 4. Primers for detecting the mutant alleles are presented in Figure 4a. Mutant mice carrying 1016 bp deletion were confirmed by PCR and Sanger sequencing (Figure 4b). We found that the testis size, weight, and histology of KO males were comparable to those of the control mice (Figure 4c–4e). In addition, there were no significant differences between the control and KO males in sperm morphology and the percentage of motile spermatozoa (Figure 4f and 4g).

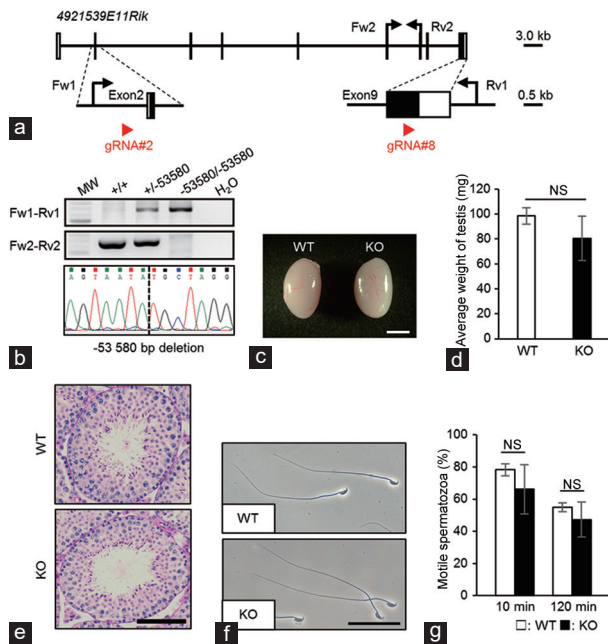


Figure 2: Phenotypic analysis of *4921539E11Rik* KO male mice. (a) KO strategy of *4921539E11Rik*. Two gRNAs (#2 and #8) were designed to target intron 1 and exon 9. Fw1/2: forward primers for genotyping; Rv1/2: reverse primers for genotyping. (b) Genotyping of *4921539E11Rik* KO mice through PCR using primer sets Fw1-Rv1 and Fw2-Rv2, and subsequent Sanger sequencing. MW: molecular weight marker. (c) Comparison of testis size between WT and *4921539E11Rik* KO mice. Scale bar = 3 mm. (d) Average testicular weight. Number of males = 3 each. (e) Histological analysis of testes in WT and *4921539E11Rik* KO mice. Scale bar = 100 μ m. (f) Spermatozoa collected from the cauda epididymis of WT and *4921539E11Rik* KO mice. Scale bar = 50 μ m. (g) Percentages of motile spermatozoa in WT and *4921539E11Rik* KO mice. Sperm motility was measured at 10 min and 120 min after incubation in TYH medium. Number of males = 3 each. KO: knockout; WT: wild type; NS: not significant.

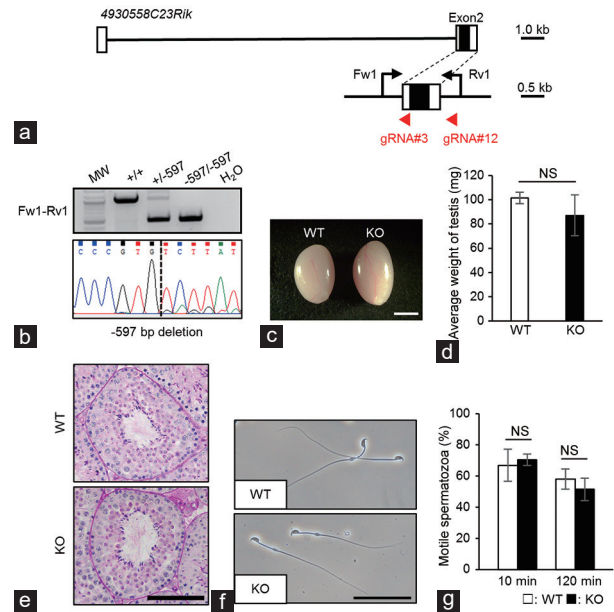


Figure 3: Phenotypic analysis of *4930558C23Rik* KO male mice. (a) KO strategy of *4930558C23Rik*. Two gRNAs (#3 and #12) were designed to target before and after the protein-coding region. Fw1: forward primer for genotyping; Rv1: reverse primer for genotyping. (b) Genotyping of *4930558C23Rik* KO mice through PCR using primer sets Fw1-Rv1 and subsequent Sanger sequencing. MW: molecular weight marker. (c) Comparison of testis size between WT and *4930558C23Rik* KO mice. Scale bar = 3 mm. (d) Average testicular weight. Number of males = 3 each. (e) Histological analysis of testes in WT and *4930558C23Rik* KO mice. Scale bar = 100 μ m. (f) Spermatozoa collected from the cauda epididymis of WT and *4930558C23Rik* KO mice. Scale bar = 50 μ m. (g) Percentages of motile spermatozoa in WT and *4930558C23Rik* KO mice. Sperm motility was measured at 10 min and 120 min after incubation in TYH medium. Number of males = 3 each. KO: knockout; WT: wild type; NS: not significant.

Fertility results of 12 testis-enriched KO mouse models

To examine the fertility of the KO males, the mice were caged with one-to-three WT females for more than 8 weeks (except for *Smim8*). We observed more than 13 deliveries, and all the KO males were able to sire normal numbers of pups during the mating period. There were no significant differences in average litter size between the control and KO males (Table 2).

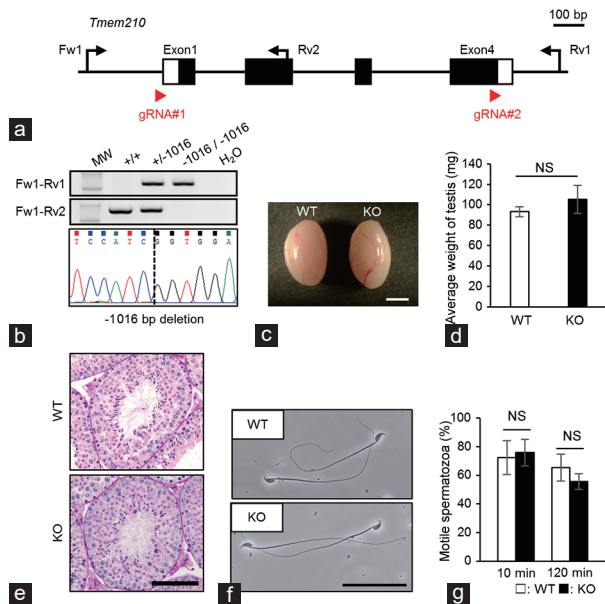


Figure 4: Phenotypic analysis of *Tmem210* KO male mice. (a) KO strategy of *Tmem210*. Two gRNAs (#1 and #2) were designed to target within the 5'-UTR and within exon 4. Fw1: forward primer for genotyping; Rv1/Rv2: reverse primers for genotyping. (b) Genotyping of *Tmem210* KO mice through PCR using primer sets Fw1-Rv1 and Fw1-Rv2 and subsequent Sanger sequencing. MW: molecular weight marker. (c) Comparison of testis size between WT and *Tmem210* KO mice. Scale bar = 3 mm. (d) Average testicular weight. Number of males = 3 each. (e) Histological analysis of testes in WT and *Tmem210* KO mice. Scale bar = 100 μ m. (f) Spermatozoa collected from the cauda epididymis of WT and *Tmem210* KO mice. Scale bar = 50 μ m. (g) Percentages of motile spermatozoa in WT and *Tmem210* KO mice. Sperm motility was measured at 10 min and 120 min after incubation in TYH medium. Number of males = 3 each. *Tmem210*: transmembrane protein 210; KO: knockout; WT: wild type; NS: not significant.

DISCUSSION

Approximately 15% of couples face the problem of infertility. While it is estimated that half of the cases are attributed to the male,² much of the pathogenic mechanisms underlying the male factor have not been clarified.²⁷ Screening genes that play essential roles in male reproduction using mouse models have led to a profound increase in our understanding of the etiology of male infertility.^{10,28} In this study, we mutated 12 genes in mice and found that these 12 genes are not essential, at least individually, for male fertility, suggesting that these genes may also not play critical roles in human male reproduction. Using this rapid CRISPR/Cas9 approach, we have reported over the past 5 years that 125 testis-restricted or epididymis-enriched genes are not essential for male fertility.^{8,11-15,25} Thus, this new study with an additional 12 genes adds to the growing list of proteins that are not feasible targets for male contraceptives.

Among the genes that we analyzed in this study, the functions of some of their paralogs have already been previously reported. For example, *Chibby family member 1 (Cby1)*, a paralog of *Cby2*, has been reported to be involved in intraflagellar transport (IFT) in cilia.²⁹ IFT is a bidirectional transport of protein complexes along axonemal microtubules, which is essential for the formation of cilia and sperm flagella.³⁰ Tracheal epithelial cells lacking *Cby1* show abnormal intracellular localization of IFT88 and IFT20.²⁹ Because depletion of IFT88 or IFT20 causes abnormal formation of sperm axoneme and male infertility,^{31,32} *Cby2* that is expressed predominantly in the testis was hypothesized to be essential for IFT in sperm axoneme and male fertility. However, we reveal that *Cby2* KO male mice are fertile. Because the expression database suggests that *Cby1* and *Cby3* are also expressed in the testis, these paralogs may function in a compensatory manner.

SLC25 family proteins are localized to the inner mitochondrial membrane and play roles in transporting solutes across the inner membrane.³³ It has been reported that solute carrier family 25 member 2 (SLC25A2) transports arginine, lysine, ornithine, and asymmetric dimethyl L-arginine,³⁴ while solute carrier family 25 member 41 (SLC25A41) transports ATP-Mg/Pi.³⁵ Translocase of outer mitochondrial membrane 20-like (TOMM20L) is also predicted to be a mitochondrial protein that is localized in the outer membrane because of its sequence similarity to TOMM20, a mitochondrial outer membrane marker.³⁶ SLC25A2, SLC25A41, and TOMM20L are all listed

Table 2: Male fertility of the 12 mutant mouse lines

Gene symbol	Genotype	Average litter size, mean \pm s.d.	Number of males	Number of delivery	Number of pups	Number of plugs	Mating period (week)
	Wild type	8.2 \pm 2.0	3	25	214	25	8
<i>1700057G04Rik</i>	-3950/-3950	7.7 \pm 1.1	4	19	145	ND	16-21
<i>4921539E11Rik</i>	-53580/-53580	8.8 \pm 2.4	3	24	210	30	8
<i>4930558C23Rik</i>	-597/-597	7.4 \pm 2.1	3	16	119	24	8
<i>Cby2</i>	-10210/-10210	8.7 \pm 2.4	3	24	209	29	8
<i>Ldhal6b</i>	-1281/-1281	9.1 \pm 1.9	3	25	227	28	8
<i>Rasef</i>	-63153/-63153	8.8 \pm 2.4	3	19	168	23	8
<i>Slc25a2</i>	-795+1/-795+1	9.3 \pm 1.8	3	20	185	24	8
<i>Slc25a41</i>	-8811/-8811	9.7 \pm 1.8	3	24	232	28	8
<i>Smim8</i>	-2300/-2300	9.4 \pm 1.4	4	16	151	16	6
<i>Smim9</i>	-12405/-12405	8.4 \pm 2.4	3	13	109	13	8
<i>Tmem210</i>	-1016/-1016	8.5 \pm 1.8	3	22	187	28	8
<i>Tomm20l</i>	-483/-483	8.0 \pm 0.5	3	15	120	ND	17-22

Statistical analysis of average litter size between WT and each KO mouse strain was performed by Welch's *t*-test for unpaired observations and there was no significant difference. *Cby2*: chibby family member 2; *Ldhal6b*: lactate dehydrogenase A-like 6B; *Rasef*: RAS and EF hand domain containing; *Slc25a2*: solute carrier family 25 member 2; *Slc25a41*: solute carrier family 25 member 41; *Smim8*: small integral membrane protein 8; *Smim9*: small integral membrane protein 9; *Tmem210*: transmembrane protein 210; *Tomm20l*: translocase of outer mitochondrial membrane 20-like; s.d.: standard deviation; ND: not determined; WT: wild type; KO: knockout

in the MitoCarta3.0 that is an inventory of genes encoding proteins with strong support of mitochondrial localization.³⁷ Mammalian spermatozoa possess the mitochondrial sheath that is localized in the midpiece of the flagella to provide structural support.³⁸ Furthermore, sperm mitochondria are suggested to be involved in various sperm functions such as sperm motility, hyperactivation, sperm capacitation, and acrosome reaction,³⁹ and disruption of mitochondrial sheath leads to male infertility.⁴⁰ Since *Slc25a2*, *Slc25a41*, and *Tomm20l* are highly expressed in the testis, we hypothesized that these genes might be involved in sperm mitochondrial function. However, our functional analyses reveal that the individual ablation of these genes does not impair male fertility.

We also mutated proteins that may have enzymatic activities. RAS and EF hand domain containing (*Rasef*) was identified as a Rab GTPase with specific expression in mouse testis.⁴¹ Rab GTPase hydrolyzes GTP to GDP and controls intracellular membrane trafficking. LDHAL6B is a homolog of LDHA that catalyzes the conversion of L-lactate to pyruvate, which is involved in glycolysis.⁴² LDHAL6B is also listed in the mitochondrial protein inventory, MitoCarta3.0.³⁷ 1700057G04Rik is a homolog of PLSCR1 that catalyzes redistribution of plasma membrane phospholipids between the inner and outer leaflets.⁴³ In addition to these genes, we found five more genes that were not essential for male fertility: *4921539E11Rik* without a known functional domain, *4930558C23Rik* containing a cortexin domain,⁴⁴ *Smim8* and *Smim9* each containing one transmembrane domain, and *Tmem210* containing two transmembrane domains.

In summary, we identified 12 genes that are not essential for male fertility in mice. We focused purely on pups sired as an assessment of male fertility in 9/12 lines and did not investigate testis histology or sperm function. Therefore, there might be subtle abnormalities in sperm structure or function in these lines that do not affect fertility. All lines will be available as bioresources, which can be analyzed further by other researchers. Recent developments in sequencing technology such as whole exome sequencing make it possible to identify causative genes of human male infertility within a short period of time.^{45–47} In the event that whole exome sequencing of infertile men reveals mutations in these 12 genes, these genes may be deprioritized and emphasis places on other potentially causative gene mutations or agents.

CONCLUSION

In this study, we generated KO mice for 12 testis-enriched genes using the CRISPR/Cas9 system. The KO mice displayed normal fertility, suggesting that these 12 genes are dispensable for male fertility, at least when individually ablated in mice. This report is anticipated to prevent unnecessary duplicative effort in generating KO mice with no apparent phenotypes.

AUTHOR CONTRIBUTIONS

All authors designed the study and analyzed the data. YO, HM, KS, YF, KT, and TXG performed experiments. YO, HM, and MI wrote the manuscript draft. All authors revised, read, and approved the final manuscript.

COMPETING INTERESTS

All authors declared no competing interests.

ACKNOWLEDGMENTS

We thank the Biotechnology Research and Development (nonprofit organization) and Naoko Nagasawa for technical support and the Department of Experimental Genome Research and Animal Resource Center for Infectious Diseases for creating a perfect environment for these experiments. This work

was supported by the Ministry of Education, Culture, Sports, Science, and Technology (MEXT)/Japan Society for the Promotion of Science (JSPS) KAKENHI grants (JP17H04987 to HM, JP20K16107 to KS, JP20KK0155 to YF, JP20K06476 to KT, and JP19H05750, JP21H04753, and JP21H05033 to MI); Japan Agency for Medical Research and Development (AMED) grant JP21gm5010001 to MI; Takeda Science Foundation grants to HM, YF, KT, and MI; Senri Life Science Foundation grant to YF; Mochida Memorial Foundation for Medical and Pharmaceutical Research grant to YF; The Sumitomo Foundation Grant for Basic Science Research Projects to YF and KT; The Ichiro Kanehara Foundation Grant to KT; Kanzawa Medical Research Foundation Grant to KT; Eunice Kennedy Shriver National Institute of Child Health and Human Development (grants R01HD088412 and P01HD087157 to MMM and MI and grant R01HD095341 to TXG); and the Bill & Melinda Gates Foundation (INV-001902 to MMM and MI).

Supplementary Information is linked to the online version of the paper on the *Asian Journal of Andrology* website.

REFERENCES

- Dada R, Thilagavathi J, Venkatesh S, Esteves SC, Agarwal A. Genetic testing in male infertility. *Open Reprod Sci J* 2011; 3: 42–56.
- Agarwal A, Mulgund A, Hamada A, Chyatte MR. A unique view on male infertility around the globe. *Reprod Biol Endocrinol* 2015; 13: 37.
- Eddy EM, Toshimori K, O'Brien DA. Fibrous sheath of mammalian spermatozoa. *Microsc Res Tech* 2003; 61: 103–15.
- Lehti MS, Sironen A. Formation and function of sperm tail structures in association with sperm motility defects. *Biol Reprod* 2017; 97: 522–36.
- Miyata H, Morohoshi A, Ikawa M. Analysis of the sperm flagellar axoneme using gene-modified mice. *Exp Anim* 2020; 69: 374–81.
- Abbasi F, Miyata H, Ikawa M. Revolutionizing male fertility factor research in mice by using the genome editing tool CRISPR/Cas9. *Reprod Med Biol* 2017; 17: 3–10.
- Schultz N, Hamra FK, Garbers DL. A multitude of genes expressed solely in meiotic or postmeiotic spermatogenic cells offers a myriad of contraceptive targets. *Proc Natl Acad Sci U S A* 2003; 100: 12201–6.
- Miyata H, Castaneda JM, Fujihara Y, Yu Z, Archambeault DR, *et al*. Genome engineering uncovers 54 evolutionarily conserved and testis-enriched genes that are not required for male fertility in mice. *Proc Natl Acad Sci U S A* 2016; 113: 7704–10.
- Uhlén M, Fagerberg L, Hallström BM, Lindskog C, Oksvold P, *et al*. Proteomics. Tissue-based map of the human proteome. *Science* 2015; 347: 6220.
- Matzuk MM, Lamb DJ. The biology of infertility: research advances and clinical challenges. *Nat Med* 2008; 14: 1197–213.
- Lu Y, Oura S, Matsumura T, Oji A, Sakurai N, *et al*. CRISPR/Cas9-mediated genome editing reveals 30 testis-enriched genes dispensable for male fertility in mice. *Biol Reprod* 2019; 101: 501–11.
- Holcomb RJ, Oura S, Nozawa K, Kent K, Yu Z, *et al*. The testis-specific serine proteases PRSS44, PRSS46, and PRSS54 are dispensable for male mouse fertility. *Biol Reprod* 2020; 102: 84–91.
- Park S, Shimada K, Fujihara Y, Xu Z, Shimada K, *et al*. CRISPR/Cas9-mediated genome-edited mice reveal 10 testis-enriched genes are dispensable for male fecundity. *Biol Reprod* 2020; 103: 195–204.
- Sun J, Lu Y, Nozawa K, Xu Z, Morohoshi A, *et al*. CRISPR/Cas9-based genome editing in mice uncovers 13 testis- or epididymis-enriched genes individually dispensable for male reproduction. *Biol Reprod* 2020; 103: 183–94.
- Robertson MJ, Kent K, Tharp N, Nozawa K, Dean L, *et al*. Large-scale discovery of male reproductive tract-specific genes through analysis of RNA-seq datasets. *BMC Biol* 2020; 18: 103.
- Fujihara Y, Lu Y, Noda T, Oji A, Larasati T, *et al*. Spermatozoa lacking Fertilization Influencing Membrane Protein (FIMP) fail to fuse with oocytes in mice. *Proc Natl Acad Sci U S A* 2020; 117: 9393–400.
- Noda T, Lu Y, Fujihara Y, Oura S, Koyano T, *et al*. Sperm proteins SOF1, TMEM95, and SPACA6 are required for sperm-oocyte fusion in mice. *Proc Natl Acad Sci U S A* 2020; 117: 11493–502.
- Lamas-Toranzo I, Hamze JG, Bianchi E, Fernández-Fuertes B, Pérez-Cerezales S, *et al*. TMEM95 is a sperm membrane protein essential for mammalian fertilization. *Elife* 2020; 9: e53913.
- Inoue N, Ikawa M, Isotani A, Okabe M. The immunoglobulin superfamily protein Izumo is required for sperm to fuse with eggs. *Nature* 2005; 434: 234–8.
- Kim D, Langmead B, Salzberg SL. HISAT: a fast spliced aligner with low memory requirements. *Nat Methods* 2015; 12: 357–60.
- Risso D, Ngai J, Speed TP, Dudoit S. Normalization of RNA-seq data using factor analysis of control genes or samples. *Nat Biotechnol* 2014; 32: 896–902.
- Robinson MD, McCarthy DJ, Smyth GK. edgeR: a Bioconductor package for differential expression analysis of digital gene expression data. *Bioinformatics*



- 2010; 26: 139–40.
- 23 Naito Y, Hino K, Bono H, Ui-Tei K. CRISPRdirect: software for designing CRISPR/Cas guide RNA with reduced off-target sites. *Bioinformatics* 2015; 31: 1120–3.
- 24 Abbasi F, Miyata H, Shimada K, Morohoshi A, Nozawa K, *et al*. RSPH6A is required for sperm flagellum formation and male fertility in mice. *J Cell Sci* 2018; 191: jcs221648.
- 25 Noda T, Sakurai N, Nozawa K, Kobayashi S, Devlin DJ, *et al*. Nine genes abundantly expressed in the epididymis are not essential for male fecundity in mice. *Andrology* 2019; 7: 644–53.
- 26 Muro Y, Hasuwa H, Isotani A, Miyata H, Yamagata K, *et al*. Behavior of mouse spermatozoa in the female reproductive tract from soon after mating to the beginning of fertilization. *Biol Reprod* 2016; 94: 80.
- 27 Oud MS, Ramos L, O'Bryan MK, McLachlan RI, Okutman Ö, *et al*. Validation and application of a novel integrated genetic screening method to a cohort of 1,112 men with idiopathic azoospermia or severe oligozoospermia. *Hum Mutat* 2017; 38: 1592–605.
- 28 Kent K, Johnston M, Strump N, Garcia TX. Toward development of the male pill: a decade of potential non-hormonal contraceptive targets. *Front Cell Dev Biol* 2020; 8: 61.
- 29 Siller SS, Burke MC, Li FQ, Takemaru K. Chibby functions to preserve normal ciliary morphology through the regulation of intraflagellar transport in airway ciliated cells. *Cell Cycle* 2015; 14: 3163–72.
- 30 Inaba K, Mizuno K. Sperm dysfunction and ciliopathy. *Reprod Med Biol* 2016; 15: 77–94.
- 31 San Agustin JT, Pazour GJ, Witman GB. Intraflagellar transport is essential for mammalian spermiogenesis but is absent in mature sperm. *Mol Biol Cell* 2015; 26: 4358–72.
- 32 Zhang Z, Li W, Zhang Y, Zhang L, Teves ME, *et al*. Intraflagellar transport protein IFT20 is essential for male fertility and spermiogenesis in mice. *Mol Biol Cell* 2016; 27: 3705–16.
- 33 Ruprecht JJ, Kunji ER. The SLC25 mitochondrial carrier family: structure and mechanism. *Trends Biochem Sci* 2020; 45: 244–58.
- 34 Porcelli V, Longo A, Palmieri L, Closs EI, Palmieri F. Asymmetric dimethylarginine is transported by the mitochondrial carrier SLC25A2. *Amino Acids* 2016; 48: 427–36.
- 35 Traba J, Satrústegui J, del Arco A. Characterization of SCA3-like/slc25a41, a novel calcium-independent mitochondrial ATP-Mg/Pi carrier. *Biochem J* 2009; 418: 125–33.
- 36 Baker MJ, Frazier AE, Gulbis JM, Ryan MT. Mitochondrial protein-import machinery: correlating structure with function. *Trends Cell Biol* 2007; 17: 456–64.
- 37 Rath S, Sharma R, Gupta R, Ast T, Chan C, *et al*. MitoCarta3.0: an updated mitochondrial proteome now with sub-organelle localization and pathway annotations. *Nucleic Acids Res* 2021; 49: D1541–7.
- 38 Ho HC, Wey S. Three dimensional rendering of the mitochondrial sheath morphogenesis during mouse spermiogenesis. *Microsc Res Tech* 2007; 70: 719–23.
- 39 Moraes CR, Meyers S. The sperm mitochondrion: organelle of many functions. *Anim Reprod Sci* 2018; 194: 71–80.
- 40 Shimada K, Park S, Miyata H, Yu Z, Morohoshi A, *et al*. ARMC12 regulates spatiotemporal mitochondrial dynamics during spermiogenesis and is required for male fertility. *Proc Natl Acad Sci U S A* 2021; 118: e2018355118.
- 41 Kumar S, Lee HJ, Park HS, Lee K. Testis-specific GTPase (TSG): an oligomeric protein. *BMC Genomics* 2016; 17: 792.
- 42 Feng Y, Xiong Y, Qiao T, Li X, Jia L, *et al*. Lactate dehydrogenase A: a key player in carcinogenesis and potential target in cancer therapy. *Cancer Med* 2018; 7: 6124–36.
- 43 Sahu SK, Gummadi SN, Manoj N, Aradhyam GK. Phospholipid scramblases: an overview. *Arch Biochem Biophys* 2007; 462: 103–14.
- 44 Coulter PM 2nd, Bautista EA, Margulies JE, Watson JB. Identification of cortexin: a novel, neuron-specific, 82-residue membrane protein enriched in rodent cerebral cortex. *J Neurochem* 1993; 61: 756–9.
- 45 Nsota Mbango JF, Coutton C, Arnoult C, Ray PF, Touré A. Genetic causes of male infertility: snapshot on morphological abnormalities of the sperm flagellum. *Basic Clin Androl* 2019; 29: 2.
- 46 Liu C, Miyata H, Gao Y, Sha Y, Tang S, *et al*. Bi-allelic *DNAH8* variants lead to multiple morphological abnormalities of the sperm flagella and primary male infertility. *Am J Hum Genet* 2020; 107: 330–41.
- 47 Xin A, Qu R, Chen G, Zhang L, Chen, *et al*. Disruption in *ACTL7A* causes acrosomal ultrastructural defects in human and mouse sperm as a novel male factor inducing early embryonic arrest. *Sci Adv* 2020; 6: eaaz4796.

This is an open access journal, and articles are distributed under the terms of the Creative Commons Attribution-NonCommercial-ShareAlike 4.0 License, which allows others to remix, tweak, and build upon the work non-commercially, as long as appropriate credit is given and the new creations are licensed under the identical terms.

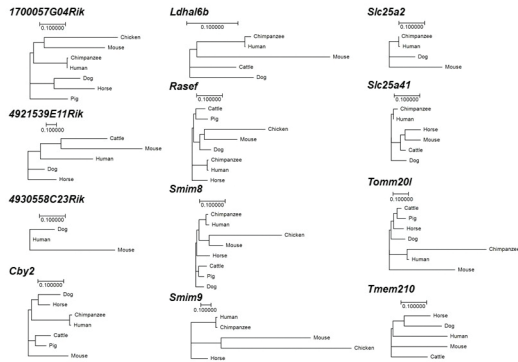
©The Author(s)(2021)

Supplementary Table 1: Primer sequences and conditions used for RT-PCR of *Ldhal6b* and *Smim9*

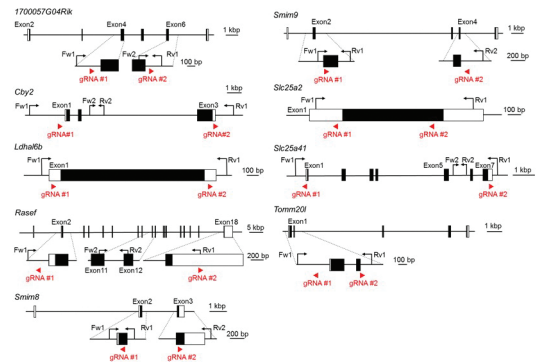
Gene symbol	Primer set for WT	Annealing condition	Elongation condition	Band size (bp)
<i>Ldhal6b</i>	Fw: GAAGAGCCCGTTCTCCACAA	65°C	72°C	504
	Rv: AGAGTGGATCCCAAGCCTCT	30 s	30 s	
<i>Smim9</i>	Fw: ATGAAGCCTCTGAAGCTGTTCTGC	60°C	72°C	414
	Rv: TCACCCACCAAAAAGCTTG	30 s	30 s	
<i>Actb</i>	Fw: CATCCGTAAGACCTCTATGCCAAC	60°C	72°C	171
	Rv: ATGGAGCCACCGATCCACA	30 s	30 s	

Supplementary Table 2: Primers and PCR conditions used for genotyping

Gene symbol	Primer set for WT	Annealing condition	Elongation condition	Band size (bp)	Primer set for KO
<i>1700057G04Rik</i>	Fw2: GGCAGGATTTCCAAGCACTG	58°C	72°C	362	Fw1: CTACCCATGCAGCTGTCC
	Rv1: GACAACCTCAGAGCTAGGGC	30 s	30 s		Rv1: (as WT)
<i>4921539E11Rik</i>	Fw2: CAGCGGAGTCTTCAGTCCCG	60°C	72°C	667	Fw1: TCCCAATGGAGGAGCTAGAG
	Rv2: GTGACCTAAGCTTGATACCC	30 s	30 s		Rv1: GAGATGGCTCATCCTGGAAA (as WT)
<i>4930558C23Rik</i>	Fw1: CTGTGACGTCCAGCTGACC	65°C	72°C	1104	
	Rv1: TGTCATAGAGCTCCACCC	30 s	60 s		
<i>Cby2</i>	Fw2: AGCAGCCACTTTCCTGTCTC	60°C	72°C	593	Fw1: ACAGGGCTGAACCCCTAACT
	Rv2: AGAGCTGGGGATGGAATCT	30 s	30 s		Rv1: TGCACCATCATACCTGCTA (as WT)
<i>Ldhal6b</i>	Fw1: AAGAAGACCCAGTCTGTGCG	65°C	72°C	311	
	Rv1: TATGCATGTGAGCCACCCAG	30 s	45 s		
<i>Rasef</i>	Fw2: CAATGAGTGTGACTCCGAGG	60°C	72°C	429	Fw1: AAACCTTAGCCTAGTAATGTTGG
	Rv2: TCTTCATCCCTTATATCTGG	30 s	30 s		Rv1: ACAGGATAATTACAACTACAGG
<i>Smim8</i>	Fw1: CCCAGGGCTCTGTGAGTTCAAGG	65°C	72°C	616	Fw1: (as WT)
	Rv1: CAAGGGCTAGGATTATAGGTGCGTGCC	30 s	30 s		Rv2: GCCTTCAGCTGTAATGAGACTAACTCACCAC
<i>Smim9</i>	Fw1: CACGACGACGGTGAGGGTTATGC	65°C	72°C	573	Fw1: (as WT)
	Rv1: GCTACCTTTGTGAAACCTTCCCTTAATCCAC	30 s	30 s		Rv2: CCAAATTCCTGCCTCCTTGTGTGC (as WT)
<i>Slc25a2</i>	Fw1: GGCTTTGGTTTGAGTAGCCT	65°C	72°C	452	
	Rv1: CTGTAGATCCCACCACCAGC	30 s	45 s		
<i>Slc25a41</i>	Fw2: TGCTCTCCTCCTCTCTCC	65°C	72°C	591	Fw1: CGTGGAGCTCATCTGCTAGG
	Rv2: GGGCCACGAAGAAGGAAGAA	30 s	30 s		Rv1: ATACACCCCATCTCCAGCT
<i>Tmem210</i>	Fw1: TCCTCTGCTTGCCTCAATCT	60°C	72°C	809	Fw1: (as WT)
	Rv2: GGCCGAAAGACCCAAT	30 s	30 s		Rv1: GTCCTGTCTTGGGAATCTG (as WT)
<i>Tomm20l</i>	Fw1: ATAAAGGGAAAAGCACCGGC	58°C	72°C	799	
	Rv1: AATGTGTCCTTACCAGACCCA	30 s	30 s		



Supplementary Figure 1: Phylogenetic analysis of the 12 testis-enriched genes in mammals and birds.



Supplementary Figure 2: KO strategy showing the location of gRNAs and genotyping primers. KO: knockout.